

How do neural connectivity and time delays influence bimanual coordination?

Arpan Banerjee¹, Viktor K. Jirsa¹²³

¹ Center for Complex Systems & Brain Sciences, Florida Atlantic University, Boca Raton, Florida 33431, USA

² CNRS, UMR 6152 Mouvement et Perception, 13288 Marseille cedex 9, France

³ Department of Physics, Florida Atlantic University, Boca Raton, Florida 33431, USA

The date of receipt and acceptance will be inserted by the editor

Abstract Multilevel crosstalk as a neural basis for motor control has been widely discussed in the literature. Since no natural process is instantaneous, any crosstalk model should incorporate time delays, which are known to induce temporal coupling between functional elements and stabilize or destabilize a particular mode of coordination. In this article, we systematically study the dynamics of rhythmic bimanual coordination under the influence of varying connection topology as realized by callosal fibers, cortico-thalamic projections, and crossing peripheral fibers. Such connectivity contributes to various degrees of neural crosstalk between the effectors which we continuously parameterize in a mathematical model. We identify the stability regimes of bimanual coordination as a function of the degree of neural crosstalk, movement amplitude and the time delays involved due to signal processing. Prominent examples include explanations of the decreased stability of the antiphase mode of coordination in split brain patients and the role of coupling in mediating bimanual coordination.

1 Introduction

The literature on the neural basis of bimanual coordination has mainly been dominated by three concepts. The generalized motor program (GMP) (Bernstein (1967); Schmidt (1975)) hypothesis states the existence of a single unified motor plan for limb movements, which is executed by the central nervous system. A second hypothesis on intermanual crosstalk (Swinnen (2002); Cardoso de Oliveira (2002)) assumes that two independent motor plans exist and that the coordination dynamics between the two end-effectors (limbs) is controlled by their crosstalk, which is defined as the interaction between different functional elements (Gerloff and Andres

(2002)) at multiple levels of organization. Functional elements are characterized by state variables such as finger movement position or electrochemical activity in muscles and brain tissues and play a functional role. Finally, the dynamic systems approach (Kelso (1995)) aims to identify general laws of pattern formation in human movements rather than searching for a locus of movement pattern generation. Such laws are expressed by a low-dimensional dynamics of so-called order parameters (Haken (1983)), also sometimes referred to as collective variables (Kelso (1995)), inspired by ideas seeded in the theory of self-organization and Synergetics (Haken (1983); Kelso (1995)). The order parameter dynamics can be rigorously obtained by a bottom-up construction from its high-dimensional microscopic equations using time-scale hierarchies (Haken (1983)). The top-down approach takes the opposite route and assumes the existence of a low-dimensional order parameter dynamics. It aims to identify the order parameter dynamics phenomenologically without knowledge of the underlying microscopic dynamics. The identification of the order parameters is guided by characteristics displayed close to transition points such as a slow characteristic time scale, critical fluctuations and critical slowing down. A classic example is the task of rhythmic bimanual coordination (Kelso (1981)) in movement sciences: under instructions to increase the frequency of bimanual movements, the antiphase motion involving simultaneous flexor and extensor muscle activities, the subject's finger movements shift abruptly to an inphase mode that involves simultaneous activation of homologous muscle groups (Kelso (1981)). The relative phase between the two fingers has been interpreted as an order parameter of the system and its dynamics have been mathematically modelled using nonlinearly and instantaneously coupled ordinary differential equations (Haken et al. (1985)). Subsequent research promulgated a plethora of models to explain the neural control of bimanual coordination (Haken et al. (1985); Nagashino and Kelso (1992); Grossberg et al. (1997); Jirsa et al. (1998); Rokni et al. (2003); Daf-

Correspondence to: Arpan Banerjee, banerjee@ccs.fau.edu, tel +1(561)297-2230, postal address indicated with title.

fertshofer et al. (2005)). However, the role of time delays is overlooked in most of these crosstalk models of motor behavior without rigorous justification, despite the fact that time delay is well-known to influence the stability properties of dynamical systems in biology (MacDonald (1989)). Hugo Liepmann (1920) proposed time delays in inter-hemispheric transfer time of motor signals as a perpetuator of temporal coupling. As no natural signal transfer is instantaneous, the question arises: do the time delays in the interlimb coupling affect the qualitative dynamics of the order parameter, and consequently influence the stability of bimanual coordination? To address the aforementioned question in this article, we formulate a representative framework for neural crosstalk incorporating the concepts of dynamical systems theory under consideration of connectivity and time delay.

The idea of multilevel crosstalk (Swinnen (2002); Cardoso de Oliveira (2002)) between functional elements as a model for the neural basis of motor control dates back to 1920 (Liepmann (1920)). The interaction of functional elements in the nervous system is considered the basis of emergent cognitive functions (Bressler and Kelso (2001); Varela et al. (2001)). Such interaction involves the integration of distributed information, for instance, sensory input of multiple modalities throughout the cortex resulting in a coherent percept and globally coherent brain states (Bressler and Kelso (2001); Varela et al. (2001); Jirsa and Kelso (2003)), which have been experimentally observed by non-invasive large scale brain imaging. Neural field models (Nunez (1974); Wright and Liley (1995); Jirsa and Haken (1996, 1997); Robinson et al. (1997)) provide a possible way to formalize such large scale brain activity during cognitive and motor tasks and allow the computation of the resulting electromagnetic fields on the scalp surface (Jirsa et al. (2002)) for comparison with experimental data. The spatiotemporal dynamics of the electromagnetic patterns can be recorded by electroencephalography (EEG) and magnetoencephalography (MEG) and has been shown to be functionally meaningful. For instance, the phase transitions in bimanual finger movements find a neural correlate in phase transitions of the spatiotemporal modes from MEG recordings (Jirsa et al. (1998); Daffertshofer et al. (2005)). Both neural and behavioral signals have been shown to exhibit a linear dependence (Kelso et al. (1998); Fuchs et al. (2000); Jirsa (2004)). The interaction between these two levels is naturally characterized by signal transfer with finite conduction speeds and, inadvertently, any information exchange between functional elements must undergo a finite time delay. The effective resulting time delay will be a function of the path, or even multiple paths, a signal takes to propagate; in particular it will depend on the connectivity between two effectors and the number of processing units involved.

To answer the title question, we will take the following approach. In section 2 we will summarize some known facts on anatomical and functional connectivity

that result in crosstalk, as well as time delays involved in neural signal propagation. Then we will develop a mathematical framework in section 3 which will allow us to study systematically the coordination stability of two effectors as a function of connectivity and time delays. In section 4 we discuss the implications of our model for bimanual coordination and draw our conclusions in section 5.

2 Background on connectivity and time delays

Functional connectivity is defined as the statistical interdependence between two functional elements without explicit reference to causal effects (Sporns et al. (2004)), whereas anatomical connectivity refers to the existence of pathways. In a recent article McIntosh (2004) argued that the functional connectivity of a specific brain area is causally related to certain behavioral and cognitive states and concomitantly related to its anatomical connectivity. The experimental data gathered over the years (Brinkman and Kuypers (1972); Tuller and Kelso (1989); Franz et al. (1996); Baraldi et al. (1999); Cattaert et al. (1999); Kennerley et al. (2002)) suggest the following functional and anatomical connectivity to be relevant for bimanual coordination: for both unimanual and bimanual tasks, there is a contribution from the contralateral and the ipsilateral motor cortices (Cardoso de Oliveira et al. (2001); Rokni et al. (2003)). The contributions of contralateral and ipsilateral projections appear to be weighted (80%: Contralateral, 20%: Ipsilateral) for bimanual tasks (Cattaert et al. (1999); Cardoso de Oliveira (2002)). However, these projections may conform to a small number of connectivity schemes. A general scheme based on the neuroanatomy of anatomical connections involved in motor control is shown in Figure 1. In a recent review paper Richard Carson (2005) draws a composite picture of the connectivity associated with the neural control of limb movement.

Callosal fibers facilitate interhemispheric crosstalk between the left and the right hemispheres. Evidence in the literature (Brinkman and Kuypers (1972); Tuller and Kelso (1989); Franz et al. (1996); Kennerley et al. (2002)) elucidates their role in temporal coupling. Kennerley et al. (2002) showed split brain patients (patients suffering from epilepsy who had their corpus callosum sectioned) undergo a loss of temporal coupling between the two effectors during a bimanual coordination task. Evidence of ipsilateral inhibition via the corpus callosum has been shown recently (Rokni et al. (2003)). The peripheral fibers (not crossed at the thalamus, e.g., corticospinal pathways) also contribute to the contralateral and ipsilateral crosstalk (Cattaert et al. (1999), Cardoso de Oliveira (2002)). In addition to this, the distributed networks which run via the thalamocortical loop are thought to be responsible for considerable amounts of crosstalk (Rouiller et al. (1999); Debaere et al. (2001); Jantzen

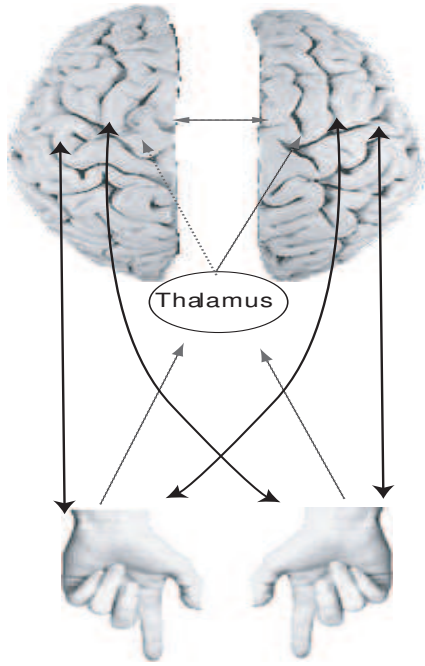


Figure 1 The anatomical pathways responsible for neural crosstalk underlying bimanual coordination. The solid lines show peripheral fibers, the dotted lines between the two hemispheres represent callosal fibers, and the dotted lines via the thalamus represent cortico-thalamic projections

et al. (2004)). Jantzen et al. (2004) showed in a functional Magnetic Resonance Imaging (fMRI) study that the activation of supplementary motor area (SMA), the cerebellum and other subcortical areas is correlated with the performance of a unimanual task in both continuation and synchronization/ syncopation paradigms. Subsequently, Daffertshofer et al. (2005) showed that the activation of ipsilateral and contralateral cortical areas in a MEG study were phase locked for a multifrequency bimanual task. The time delays associated with these pathways and their signal processing are deduced from a variety of data: interhemispheric transfer time has been estimated to be about 5ms (Halgren (2004)) based on behavioral (Clarke and Zaidel (1989), Marzi et al. (1991)) and physiological studies (Brown et al. (1999)), including intracranial recordings in humans (Clarke et al. (1999)), whereas the maximum possible delay for the cortico-thalamo-cortical loop has been estimated at about 20ms (Halgren (2004)). In most circumstances, transmission delay in the brain does not exceed 100ms (Tass (1999)). However, for the visual system it exceeds up to 150ms (Thorpe et al. (1996)).

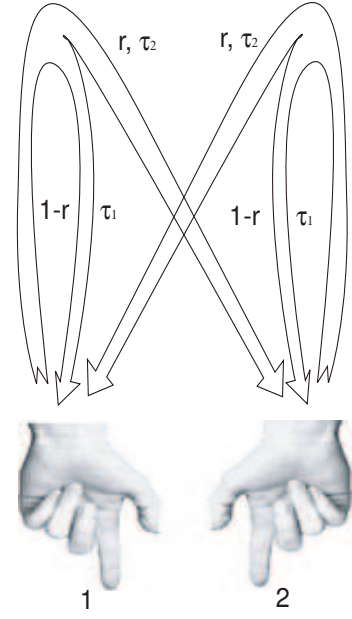


Figure 2 The simplified connection topology incorporating the key functional elements addressed by the crosstalk model. r is the strength of mutual coupling which undergoes a time delay τ_2 and $1 - r$ is the strength of self coupling which also undergoes a time delay τ_1 .

3 The dynamic crosstalk model

To develop a theoretical framework for rhythmic bimanual coordination dynamics as a function of connectivity and time delay, we present the following line of thought: for rhythmic movements it has been shown repeatedly that the effector dynamics and neural dynamics are linearly related (Georgopoulos et al. (1989); Fuchs et al. (2000); Jirsa (2004); Daffertshofer et al. (2005)), which is equivalent to a phase shift operation for periodic signals. In other words, the neural oscillations are phase locked to the frequency of bimanual finger movement. Hence, it is evident that most processes involved in this crosstalk average out all non-resonant contributions of the signal, that is, all contributions which do not oscillate with or are not modulated by the basic movement frequency. Consequently, despite that every signal which is sent from effector 1 to effector 2 will be a non-trivial function of the number of processing units and propagation times involved, the signal arriving at effector 2 can be approximated as the effector signal 1 itself, but shifted by an effective time delay τ_{12} . The same reasoning holds for signals sent to the cortex by effector 1 and returned back to effector 1 as feedback with time delay τ_{11} . More generally, if we normalize all outgoing signals of effector 1 to be the ratio r of outgoing signal sent to effector 2 over the total outgoing signal, then it follows naturally that $1 - r$ is the ratio of outgoing signal returned to the effector over the total outgoing signal. For symmetry reasons, the same coupling scheme and quantification will hold for the other effector and as a

result, $\tau_{11} = \tau_{22} = \tau_1$ and $\tau_{12} = \tau_{21} = \tau_2$. The ratio r is naturally a measure for the degree of crosstalk. An illustration of this signal weighting and connectivity is given in Figure 2. Two simplifications are in order: First, as multiple processes on various levels will be involved in the bimanual crosstalk, it is most likely that the signal arriving at the receiving effector will be dispersed in time. Dispersed time delays have been shown to be less destabilizing than a single discrete time delay (Jirsa and Ding (2004)), hence the dynamic system with a single discrete time delay will provide us with a lower bound for the stability of bimanual coordination. Second, the r weighted outgoing pathways and $1 - r$ weighted feedback pathways do not necessarily have the same time delay $\tau_1 = \tau_2 = \tau$ as indicated in Figure 2. It is not unreasonable to assume that the delays τ_1 and τ_2 are at least of similar order of magnitude due to the short inter-hemispheric delay (Halgren (2004)) and the fact that all other processes are likely to involve both outgoing and feedback pathways. Still, we keep this approximation in mind as a potential source for errors, but make for the current article the assumption $\tau_1 = \tau_2 = \tau$.

The connectivity scheme illustrated in Figure 2 may be interpreted as follows: If only peripheral ipsilateral pathways exist, then $r = 0$. If only the peripheral fibers exist and split into 80% contralateral and 20% ipsilateral contribution, then $r = 0.8$. If in addition callosal fibers are added, then r will increase towards 1. If equally weighted thalamic projections were the dominating connection topology, then r would be close to 0.5. Naturally, it is not possible to unambiguously identify the underlying connection topology from the knowledge of the degree of crosstalk quantified by r . However, it will be possible to obtain a quantitative sense about the degree of mutual interaction. It is notable that ongoing discussion in the neuroscientific literature addresses temporal changes in functional connectivity as a neural mechanism to implement attentional effects, as well as general task conditions for cognitive tasks (Friston et al. (2003); Penny et al. (2005)). If future research shows temporal changes in functional connectivity to be relevant for bimanual coordination, then such will find its implementation in a time dependent crosstalk parameter r .

3.1 Oscillator level

In a recent article Jirsa and Kelso (2005) showed that discrete and rhythmic movement dynamics can be modelled with a class of dynamic systems called "excitators". Each excitator represents an effector and can realize various task conditions by creating patterns of dynamic flow in their respective state space. Task conditions include discrete and periodic movements and are captured in general by the topology of the dynamic flows, for instance using single or multiple fixed points or limit cycles. The details of the flow determine the details of

the effector dynamics, including transient behavior, and have recently become empirically accessible through novel methods of experimental data analysis (van Mourik et al. (2006)). The dynamic flow of an effector with no coupling is referred to as the intrinsic dynamics and written as follows:

$$\begin{aligned}\dot{x} &= c(x + y - g_1(x) + I) \\ \dot{y} &= -(x - a + g_2(x, y))/c\end{aligned}\quad (1)$$

where x is the finger position and y is related to the velocity of movement (see Jirsa and Kelso (2005) for details). The dot indicates the time derivative. a and c are constant parameters and define the position of the equilibrium point and the time scale respectively. I is an external input and the functions $g_1(x), g_2(x, y)$ define the dynamic flow in the state space dependent on task. For the current study of a purely rhythmic task, we specify the flow in equation (1) such that the excitator becomes equivalent to a Van der Pol oscillator via $g_1(x) = R_0^{-2}x^3/3$ and $g_2(x, y) = 0$ where R_0 controls the amplitude of the oscillation. Note that other oscillators with sufficiently similar properties, e.g. a fifth order polynomial in g_1 or a Rayleigh oscillator, do not qualitatively change the results of our present study. The introduction of coupling through the input I of an end-effector results in the convergence or divergence of the flow in the state space (assuming weak coupling). Such convergence/divergence may be quantified by the Euclidean distance between the two trajectories and, relevant for the present study, reduces to a description of the relative phase between two coupled limit cycle oscillators (Jirsa and Kelso (2005)).

To motivate the coupling function between two end-effectors via I , as illustrated in Figure 2, we employ the following line of thought: large scale networks communicate via firing rates of the neural populations involved. The resulting synaptic input into a neural population can be split into 1) instantaneous input of local on-going population activity and 2) an external remote input which will be typically delayed. The sign of the synaptic inputs is determined by the neurotransmitters and receptors at a given synapse. The synaptic inputs linearly sum up along the dendritic trees and give rise to Local Field Potentials (LFP) (see for instance Wilson and Cowan (1972); Jirsa and Haken (1996); Roxin et al. (2005)). Equivalently, so-called electric coupling for gap junctions or axo-axonal coupling (see for instance Schmitz et al. (2001)) give rise to a similar functional form, though synaptic coupling is by far the more prevalent. For the bimanual coordination task described here, this coupling has been used previously to capture the neural dynamics observed in MEG recordings (Jirsa et al. (1998)). Another form of coupling in the firing rate modeling literature is the so-called shunting coupling established by Grossberg (1977) and also used by other authors for studies in bimanual rhythmic coordination (Grossberg et al. (1997)) and polyrhythmic movement

coordination (Daffertshofer et al. (2005)), the latter also in conjunction with MEG studies. In our current study we use a linear difference coupling in terms of the end-effector variables which nicely recovers the original equations of Haken, Kelso and Bunz (Haken et al. (1985)) as a limit case for no delay and a particular degree of crosstalk r . We write the coupling as follows with the indices $j, k = 1, 2$ and $j \neq k$

$$p(r, x_j, x_{j\tau}, x_{k\tau}) = x_j - (1 - r)x_{j\tau} - rx_{k\tau} \quad (2)$$

where $x_j \equiv x_j(t)$ denotes the instantaneous position of an effector and $x_{j\tau} \equiv x_j(t - \tau)$ the position at a previous time point $t - \tau$. The pathways as illustrated in Figure 2 are implemented through feedback as a *self delay* ($x_{j\tau}$) and *mutual delay* ($x_{k\tau}$) terms. The contribution of the self coupling is weighted by $1 - r$ and the mutual coupling is weighted by r . The coupling function p in (2) is linear and does not allow for multistability in this form. Hence we extend the final coupling function to include a cubic term in p and obtain

$$I = \epsilon(p - \frac{p^3}{3}) \quad (3)$$

where ϵ is a constant parameter. Now the coupling I has the property that if the difference term in p becomes large, then I will switch its sign and hence provides the possibility for multistable solutions by introducing convergent and divergent flows in the state space. In this sense the specific form of the nonlinear term in p plays a secondary role and a different nonlinear term of the same symmetry with regard to the exchange $p \rightarrow -p$, for instance a fifth order term $p^5/5$, yields qualitatively the same results as the cubic term. However, we rigorously presume an odd symmetry of the coupling function I . Note that in this form the coupling I in (3) reduces to the coupling used in (Haken et al. (1985)) for the limit case $\tau = 0$ and $r = 1$ and the self coupling vanishes, i.e. the crosstalk is completely mediated via the mutual coupling. In the other limit, $r = 0$, the oscillators are completely disconnected, and hence, there is no crosstalk via the mutual coupling. Our final equations then read with the indices $j, k = 1, 2$ and $j \neq k$

$$\dot{x}_j = c[y_j + x_j - R_0^{-2}\frac{x_j^3}{3} + \epsilon(p - \frac{p^3}{3})] \quad (4)$$

$$\dot{y}_j = -(x_j - a)/c \quad (5)$$

It is tempting to interpret a negative ϵ as an excitatory coupling and a positive ϵ as inhibitory (similar to neural oscillators), because for $\epsilon < 0$ the linear contribution $-(1 - r)x_{j\tau} - rx_{k\tau}$ of incoming signals increases the rate of change \dot{x}_j and, equivalently, decreases for $\epsilon > 0$. However, the total expression for the coupling I in (3) is not always positive as is the case for firing rates in neural field models, hence a clear discrimination of the nature of coupling is not possible on this level of description of end effectors. For the following sections, we will use the

notation of positive coupling for $\epsilon > 0$ and negative for $\epsilon < 0$.

Our objective is to investigate the inphase and antiphase solutions of this system (equations (4) and (5)) and the parameter regimes of their stability. Comparison of the stability regimes for certain parameter values and hence, network structures provide us with a window to infer the nature of the crosstalk at the neural level. The relative phase between the two oscillators is the collective variable of the system. At the neural level, relative phase between two oscillatory time series can be a macroscopic observable, which characterizes the synergy between the functional elements (Gray et al. (1997); Varela et al. (2001)). In the next section we show how to derive a phase level description for such a system.

3.2 Phase level

We choose the parameter values such that the system's (equations (4) and (5)) intrinsic dynamics is in the limit cycle regime with $a = 0$ and $c = 3$. Then the system can be solved by the ansatz,

$$x_j = A_j e^{i\omega t} + A_j^* e^{-i\omega t} \quad (6)$$

where the complex amplitude A_j can be time dependent, but is much slower than that of $e^{i\omega t}$ and ω is the mutual frequency. The asterisk indicates the complex conjugate. We then perform two approximations well known in the theory of nonlinear oscillators (Haken (1983)). The "slowly varying amplitude approximation" means that we may neglect the \dot{A} terms compared to terms ωA . The "rotating wave approximation" means that we may neglect terms containing $e^{3i\omega t}$ and $e^{-3i\omega t}$ compared to $e^{i\omega t}$ and $e^{-i\omega t}$. The complex amplitude A has a real and imaginary part,

$$A_j = R_j e^{i\phi_j} \quad (7)$$

where ϕ_j represents the time dependent phase and R_j the real amplitude. The real amplitude can be adiabatically eliminated (see appendix A) and expressed as

$$R_1 \approx R_2 = R_0 \quad (8)$$

We obtain the phase equation

$$\begin{aligned} \dot{\phi}_j = & \frac{1 - \omega^2}{2\omega} + \frac{\epsilon}{2} \left[\sum_{l,m=1}^2 A_{lm} \sin(2\phi_{l\tau} - \phi_{m\tau} - \phi_j) + \right. \\ & \sum_{l,m=1}^2 B_{lm} \sin(\phi_{l\tau} - \phi_{m\tau} - 2\phi_j) + C \sin(\phi_{k\tau} - \phi_{j\tau}) + \\ & \left. \sum_{l,m=1}^2 D_{lm} \sin(\phi_{l\tau} + \phi_{m\tau} - 2\phi_j) + E \sin(\phi_{j\tau} + \phi_j) \right] \quad (9) \end{aligned}$$

where $\phi_{j\tau} = \phi_j(t - \tau)$ and A_{lm} , B_{lm} and C are nonlinear functions of r and R_0 (for detailed expressions, please see appendix A). The fixed point solutions of these equations

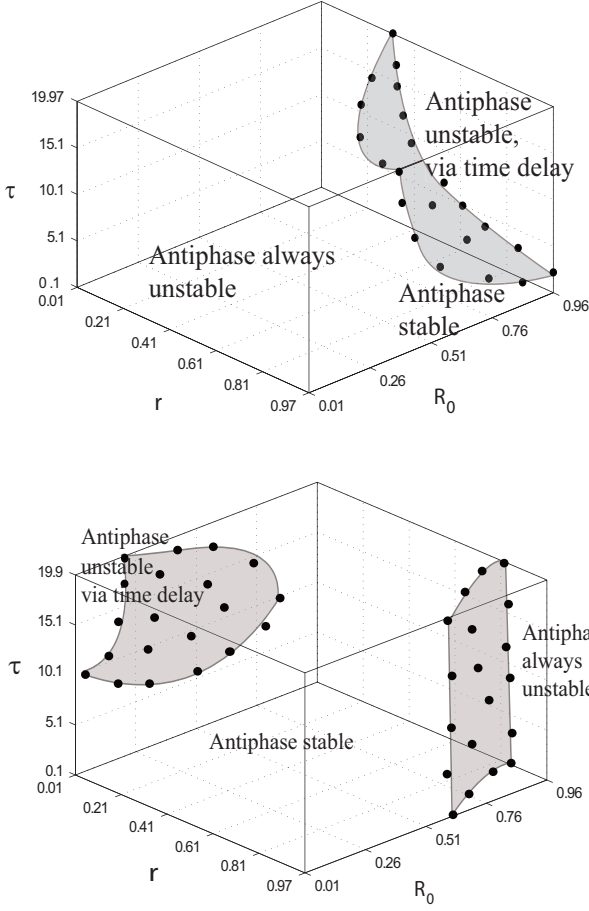


Figure 3 Boundaries of stability regimes for **antiphase** obtained numerically where a) $\epsilon = -0.2$, negative coupling, b) $\epsilon = 0.2$, positive coupling strength. The dots indicate selected points obtained from the numerical simulation.

always include multiples of π in addition to the zero solution. Other stationary solutions may exist, but will not be investigated here. The relative phase, $\phi = \phi_1 - \phi_2$, defines the inphase solutions by $\phi = 0$ or even multiples of π , and the antiphase solutions by $\phi = \pi$ or odd multiples of π . In the following, we first numerically generate the boundaries of the stability regimes for inphase and antiphase solutions and then analytically compute these regimes via linear stability analysis.

3.3 Numerical Methods:

We solved the system of equation (9) by the MATLAB solver dde23 (Shampine and Thompson (2001)) for discrete values of $r, R_0 \in [0, 1]$ and $\tau \in [0, 20]$. The solver implements a continuous extension of explicit Runge-Kutta, second and third order formulas. It interpolates the integrand function at the locations introduced by time delay between two declared grid points using a cubic Hermite polynomial (Shampine and Thompson (2001)).

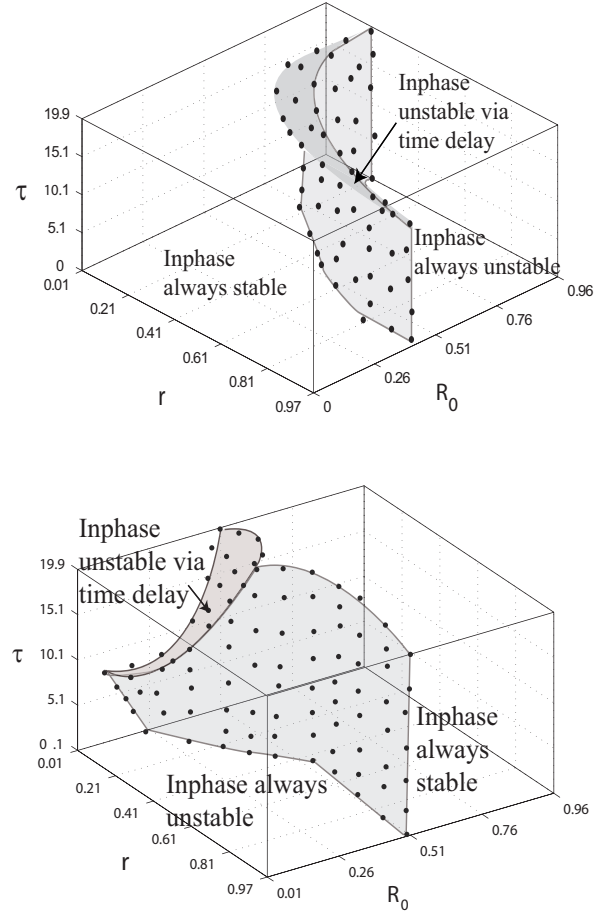


Figure 4 Boundaries of stability regimes for **inphase** obtained numerically a) $\epsilon = -0.2$, negative coupling b) $\epsilon = 0.2$, positive coupling strength. The dots indicate selected points obtained from the numerical simulation.

As ϕ_1 and ϕ_2 evolve in time and reach a stationary value, the relative phase $\phi = n\pi \pm \delta$ ($n = 0, 1, 2, \dots$) is identified as stable if it remains sufficiently long within a small interval $\delta < 0.001$.

The resulting boundary at which the stability changes occur is approximated and plotted as a surface within the three dimensional space (r, R_0, τ) in Figure 3 for antiphase and in Figure 4 for inphase. Some representative sparse points illustrate the precise location of the numerically obtained boundary. Both figures distinguish negative, $\epsilon = -0.2$, and positive, $\epsilon = 0.2$, couplings.

3.4 Linear Stability Analysis and Results

We perform a linear stability analysis around the antiphase and inphase fixed points. In general, the linearized equations are represented as follows,

$$\dot{\Phi} = \mathbf{L}_1 \Phi + \mathbf{L}_2 \Phi_\tau \quad (10)$$

where $\Phi = \begin{pmatrix} \phi_1 \\ \phi_2 \end{pmatrix}$, $\Phi_\tau = \begin{pmatrix} \phi_{1\tau} \\ \phi_{2\tau} \end{pmatrix}$, and $\mathbf{L}_1, \mathbf{L}_2$ are matrices whose elements are functions of r and R_0 . Due to symmetry properties of the matrices \mathbf{L}_1 and \mathbf{L}_2 we show in appendix B that it is always possible to obtain an independent relative phase equation

$$\dot{\phi} = L\phi + L_\tau\phi_\tau \quad (11)$$

where $\phi_\tau = \phi(t - \tau)$ and L, L_τ are nonlinear functions of r and R_0 . In appendix B, L and L_τ are computed explicitly and show a smooth dependence on r and R_0 . The stability of the delay differential equation (11) is determined by the characteristic polynomial (Hale and Lunel (1993))

$$H(z) = z - L - L_\tau e^{-z\tau} = 0 \quad (12)$$

where $\phi(t) = e^{zt}$, $z \in \mathbb{C}$ and $L, L_\tau \in \mathbb{R}$. If all the roots satisfy $\text{Re}(z) < 0$ then the solution is stable. It is easy to see that $\text{Re}(z) = 0$ is the critical value where the system destabilizes. The possibility of a change in the sign of $\text{Re}(z)$ by way of $\text{Re}(z) \rightarrow \infty$ is excluded by a theorem of Datko (1978). Hence all other sign changes of $\text{Re}(z)$ must occur at purely imaginary $z = i\Omega$, $\Omega \in \mathcal{R}_0^+$. Substituting these values in (12) we obtain the following expressions,

$$\Omega = L \tan(\Omega\tau) \quad (13)$$

$$\Omega^2 = L_\tau^2 - L^2 \quad (14)$$

Using equations (13) and (14), we obtain an expression for the critical stability surface,

$$\tau^* = \frac{1}{\sqrt{L_\tau^2 - L^2}} \tan^{-1}\left(\frac{\Omega}{L}\right) \quad (15)$$

where τ^* is the minimal delay required to destabilize the fixed point (antiphase or inphase). Jirsa and Ding (2004) proved that the roots of (12) always describe instabilities. Hence there is no possibility that the system stabilizes again for large τ . The critical surfaces, at which the instabilities occur, are plotted in figures 5 and 6. The white areas in the surface plots represent stable regions for either the antiphase or the inphase mode. The dark areas represent the critical surface above which that particular mode destabilizes. Our analytical results in figures 5 and 6 compare favorably with the fully numerical results in figures 3 and 4. Here we use a small value of coupling strength $|\epsilon| = 0.2$ as did previous authors (Haken et al. (1985); Jirsa et al. (1998)). Note that the magnitude of the coupling strength plays only a minor role because it can be mostly absorbed by a rescaling of time.

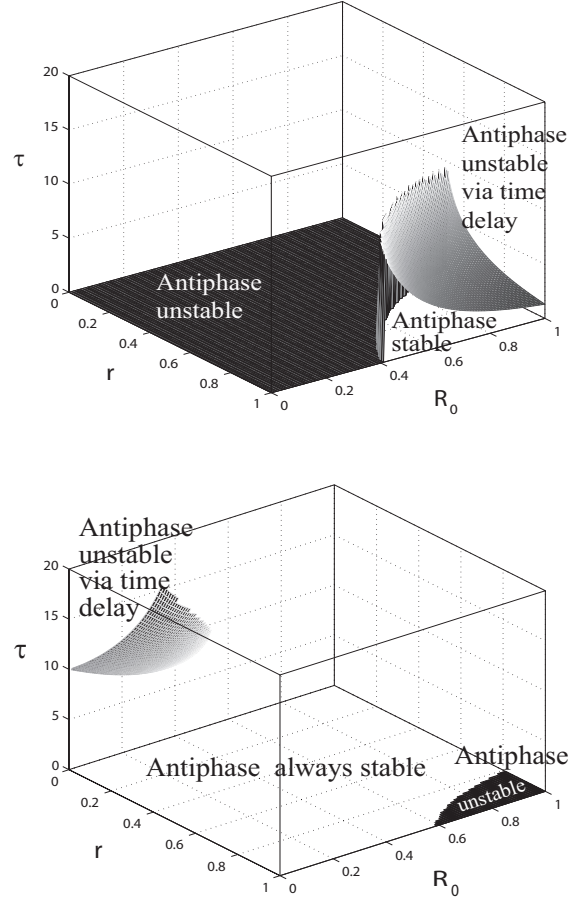


Figure 5 Critical stability surfaces for **antiphase**. The region above the surface represents instability and the region under the surface represents stability a) $\epsilon = -0.2$, for negative coupling strength b) $\epsilon = 0.2$, for positive coupling strength.

4 Discussion

4.1 Antiphase

For *negative coupling*, $\epsilon = -0.2$, Figure 5a shows that the antiphase mode of coordination is always stable independent of time delay until the degree of crosstalk, r , reaches a critical value. The antiphase solution is always unstable at low amplitude, $R_0 < 0.5$, or equivalently, high frequency for large degrees of crosstalk $r > 0.5$ and independent of time delay. In the following we use large values of R_0 interchangeably as an indicator of large amplitude or low frequency (and vice versa). In Figure 5, at low frequencies where $R_0 > 0.5$, the antiphase solution is stable for most values of r and small time delays. In this regime, where $r \geq 0.5$, the antiphase solution can be destabilized by increasing the time delay. From the critical surface shown in Figure 5a we obtain that the critical time delay value increases when the crosstalk parameter r and movement amplitude R_0 are close to the boundary values of zero delay. Hence, we can argue that stable antiphase solutions exist at low frequencies ($R_0 > 0.5$) and

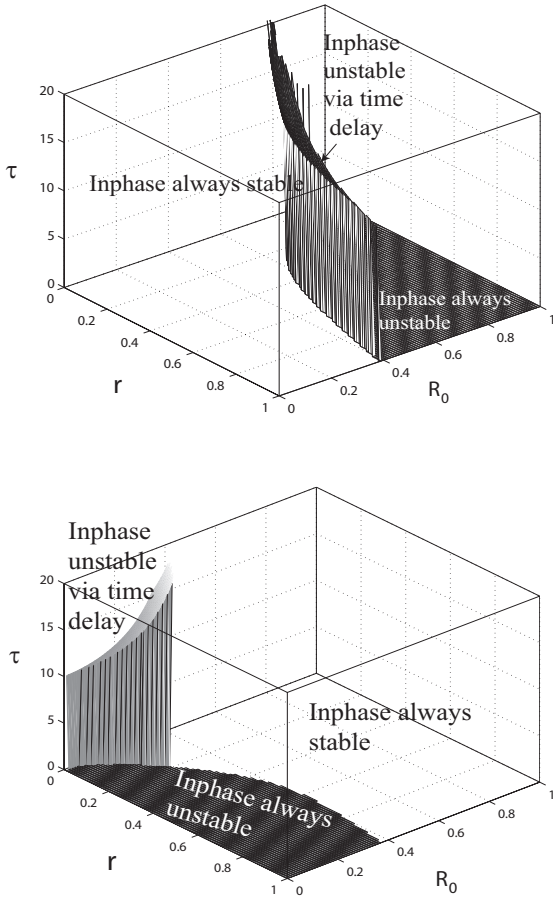


Figure 6 Critical stability surfaces for **inphase**. Here the same situation is presented as in figure 5.

the system destabilizes at higher frequencies ($R_0 < 0.5$) for values of crosstalk $r > 0.5$. This result is supported by the numerical solutions of the complete system as seen in Figure 3. When $r = 0$, the oscillators are mutually uncoupled, however, the self delayed coupling exists. In this case, antiphase mode is always unstable irrespective of the value of time delay. In the regime $r \in [0, 1]$ and $R_0 \in [0, 0.5]$ antiphase is always unstable. Hence in principle, destabilization of the antiphase mode at lower frequencies can also be understood as being due to the lower degree of crosstalk. When r is continuously decreased from $r = 1$ to $r = 0$ the mutual interaction between the effectors decreases and results in an instability. We observe a decrease in the stability of the antiphase mode in this region for all values of $R_0 \in [0, 1]$. A smaller degree of crosstalk is to be expected for lesions of neural pathways, for instance, as in a split brain patient whose corpus callosum has been surgically sectioned. This is reflected in the experimental data of Tuller and Kelso (1989), where decreased stability of the antiphase mode of coordination are observed in bimanual coordination for split brain patients. It was shown earlier by Cattaert et al. (1999) that contralateral and ipsilateral pathways

contribute to bimanual tasks with the estimates, 80% for contralateral and 20% for ipsilateral pathways. The existence of only such peripheral pathways for neural crosstalk will be characterized by a crosstalk parameter $r = 0.8$. Based on these considerations, we argue that a probable degree of crosstalk will be in the interval $r \in [0.5, 1]$ for a negative coupling scheme. As noted earlier, the HKB scenario (Haken et al. (1985)) is a special case in this regime at $r = 1$ and $\tau = 0$. A feature not considered within the HKB scenario is the effect of time delays, which is evident from Figure 5a to be relevant for destabilizing antiphase solutions. This prediction of time delay destabilizing coordination will be an entry point for us to address the question raised in the title of this article.

For *positive coupling* $\epsilon = 0.2$, the critical delay surface is plotted in Figure 5b. The surface illustrates that the antiphase mode of coordination is unstable at higher values of crosstalk parameter $r \in [0.85, 1]$ and low frequency $R_0 > 0.6$. For lower amount of crosstalk $r < 0.4$ and high frequencies $R_0 < 0.3$ antiphase can only be destabilized by increasing the time delay. Unless frequency changes are somewhat linked to time delay changes, we conclude that the overall effect of neural crosstalk must be effectively negative. The critical stability surface also suggests that the positive coupling in general is more favorable to the stabilization of the antiphase mode of coordination whereas negative coupling can be associated with destabilization of antiphase. Such a conclusion is consistent with recent experimental results (Cardoso de Oliveira et al. (2001); Rokni et al. (2003)).

4.2 Inphase

For *negative coupling* $\epsilon = -0.2$, we obtain that inphase solutions are always stable for $r < 0.1$ and all frequencies as illustrated in Figure 6a. However, they can be destabilized at low frequencies ($R_0 > 0.4$) with increasing degrees of crosstalk $r > 0.1$ and time delay $\tau > 12$. Comparing Figures 5a, 6a it is evident that the stability of antiphase requires a higher amount of crosstalk than the inphase solutions. This might be a possible explanation for the decreased stability of the antiphase mode in split brain patients who have a tendency to switch into inphase mode even if they are instructed to maintain some other specific phase relationship (Tuller and Kelso (1989)). For large degrees of crosstalk, $r \in [0.5, 1]$, and for high frequencies, $R_0 < 0.5$, antiphase is unstable and inphase stable. For the same degree of crosstalk but small frequency $R_0 > 0.4$, there is a region where inphase remains stable and antiphase becomes stable, which causes the system to be bistable, allows for hysteresis and closely resembles the experimental results (see Kelso (1995)).

For $\epsilon = 0.2$ (positive coupling), we obtain critical stability surfaces as shown in Figure 6b. Here, an HKB

like coupling scheme, $r = 1$, can lead to a destabilization of inphase at high frequencies, $R_0 < 0.35$. On the other hand, inphase can be stabilized by decreasing the degree of crosstalk, r . However, for lower values of crosstalk inphase can be destabilized via high values of time delay. Hence, it can be highlighted that inphase stabilization can occur for smaller degrees of neural crosstalk, even in a positive coupling scheme.

4.3 Parameter estimates

We estimate the relation between the computational units and the corresponding physical units of time delay in seconds following the line of thought developed by Jirsa and Kelso (2005). The time unit estimate was based on the choice for the computational angular eigenfrequency $\omega = 2\pi f = 1/T = 1$ of the oscillators (equation (9)) used in numerical solutions; where f is the frequency and T the period of a cycle. Experimentally, preferred finger movement frequencies range from around 1.1 Hz to 3.0 Hz following instructions to move the finger at a comfortable pace and through a comfortable range of motion (Jirsa and Kelso (2005)). If we identify the preferred frequency with the eigenfrequency and estimate it as 2 Hz, then one computational time unit will correspond to 80 ms or, equivalently, 12.5 computational time units will correspond to 1 s. We have studied a parameter space of $\tau \in [0, 20]$ which corresponds to $[0, 1600]$ ms. Under these conditions, the critical delay values for antiphase solutions lie in the interval $[160, 800]$ ms in a negative coupling scheme. For positive coupling, the equivalent estimate falls in $[800, 1600]$ ms. A similar analysis on inphase solutions, yield the interval $[1120, 1600]$ ms for the critical delay values in a negative coupling scheme. For positive coupling, the critical delay interval is $[800, 1600]$ ms.

5 Conclusion and Summary

Pioneered by J. A. Scott Kelso and Michael Turvey (Kugler et al. (1980); Kelso et al. (1980, 1981)), the approach of coordination dynamics is deeply connected with the bimanual rhythmic coordination paradigm, which has been used to investigate many levels of motor behavior and cognition including learning (Zanone and Kelso (1992)), attention (Temprado et al. (1999)), intention (Schöner and Kelso (1988)), social coordination (Schmidt et al. (1990)) and many more. In this article, we ask the question about the nature of the underlying substrate of bimanual coordination with its realizations in connectivity and time delays in crosstalk. Our reasoning rests heavily on the fact that neural and behavioral effects seem to be linearly related, at least for rhythmic movements. The linear dependence has been confirmed in various tasks by different researchers using a wide range of brain imaging modalities, which provides confidence in

its reality. The second foundation of our reasoning rests upon the normalized ratio r of the outgoing signals from one effector to the other. By construction, r quantifies the degree of crosstalk between both effectors. We illustrated along anatomically existing pathways, such as thalamic projections or callosal fibers, that our mathematical representation indeed captures the underlying connectivity schemes and inferred that multiple connecting pathways must be represented somewhere along the continuous interval $[0, 1]$ of r . Armed with these tools, we systematically studied the stability of coordination, which we visualized by critical surfaces as functions of the degree of crosstalk r , the time delay τ involved in the crosstalk between two effectors, and the movement frequency or, equivalently, the movement amplitude R_0 (assuming the interdependence of these two quantities following Kay et al. (1987)).

Our discussion of the stability surfaces allows us to identify mechanisms which the nervous system potentially uses to change stability of a movement behavior and hence switch from one pattern of coordination to another. In accordance with the classic line of thought, the volume element defined by $r \in [0.5, 1]$, $\tau < 800$ ms and $R_0 \in [0, 1]$ with negative overall coupling strength qualifies as a biologically realistic regime, which reproduces the established behavioral results of bistability, hysteresis and transitions from antiphase to inphase mediated by decreasing amplitude/increasing movement frequency. Within this parameter regime, the reduced degree of crosstalk r offers an attractive explanation for the decreased stability of the antiphase mode in split brain patients. Another interesting feature of split brain patients is that they spontaneously switch to inphase mode from any other relative phase relation (Tuller and Kelso (1989)). Our study indicates that a stable inphase mode of coordination requires a lesser amount of neural crosstalk and thus it can be maintained comfortably even under pathological conditions. We propose alternative approaches to regain the stability of the antiphase mode for split brain patients: the crosstalk between the effectors can be increased by either enhancing the contribution of the mutual coupling between the effectors or, equivalently, by reducing the contributions of the feedback loop for each effector. In both cases, the overall effect will be an increase in the relative degree of crosstalk r . A completely different mechanism to achieve instability and changes in coordination behavior is by varying functional connectivity, which is proposed by research in functional brain imaging (Friston et al. (2003)). In the current framework, functional connectivity is operationalized as a manipulation of the parameter r as well as by varying the time delay τ . For instance, if the decrease in movement amplitude is not causally related to the change in stability and the subsequent transition from antiphase to inphase, then an alternate route can be taken along the r axis towards smaller values of r . Under these circumstances, transitions for constant movement

amplitude can be accomplished, a phenomenon which has been observed by Peper and Beek (1999). An additional discussion of the roles of antiphase and inphase and their stability is found in the literature with regard to the manipulation of symmetries (Byblow et al. (1994); Carson et al. (2000); Lee et al. (2002)). These authors manipulated the symmetry in the experimental system such that antiphase and inphase exchanged their roles. For instance, Carson et al. (2000) systematically changed the position of the axis of a manipulandum and induced transitions from antiphase to inphase, but not in the reverse. Our discussion of the stability surfaces show that such an exchange of stability can never be accomplished by changing the coupling from negative to positive, despite the fact that this mechanism appears to be attractive, because a change from negative to positive coupling favors the stabilization of antiphase and destabilization of inphase. As evident from the comparison of the stability surfaces in figures 5a and 6b, such a change in the nature of coupling does not result in a fully symmetric exchange of the roles of antiphase and inphase, and hence is not consistent with the experimental observations. For this reason, we conclude that the approach by Jirsa and Fuchs (2000) still holds, who used a symmetry-based technique, which actually postulates a change of the coupling function rather than just the coupling strength. Finally, the discussion of the time delay provides us with an entry point toward an understanding of the effects induced by signal processing times in the nervous system. We have shown here that the introduction of a time delay into the afferent signals between coupled end-effectors does not change the form of the stationary solutions, but does affect their stability. The necessary mathematical assumptions of our study are two limit cycle oscillators which are weakly coupled via a difference coupling. The difference coupling must be of the form that it switches its sign for increasing values of the difference term and such yields the possibility for multistability. Under these conditions we provided a systematic stability analysis addressing the effects of time delay in the afferent signals as a function of the sign of ϵ and the total coupling. Our study shows that the time delays required to destabilize stationary bimanual coordination are in realistic parameter ranges, that is [160, 800] ms for the antiphase mode and [1120, 1600] ms for the inphase mode, assuming negative coupling. This supports the fact that the inphase mode of coordination is generally more stable than antiphase (see Kelso (1995)) and hence, requires higher values of time delay to destabilize. Beyond the conceptual contribution of this study, experimental support of our results may be provided by temperature-controlled changes realized in the transmission speed of peripheral fibres. Cheyne et al. (1997) conducted studies of this nature and showed evidence of generated time delays up to 100ms quantified by the event-related fields in MEG. The time delay aspect of the stability of individual modes has implications

for development, in which bimanual coordination should stabilize with increasing myelination of cortical pathways in the first years of infancy (Sampaio and Truwit (2001)) and, hence, results in reduced time delay. On the other hand, we expect that degradation of the degree of myelination, as observed in ageing or diseases such as schizophrenia (Lim et al. (1999)), should always result in reduced stability of bimanual coordination.

Acknowledgements We thank J. A. S. Kelso and Betty Tuller for inspiring discussions during preparation of the manuscript as well as Felix Almonte, Murad Qubbaj and Craig Richter for comments. We also wish to thank one anonymous reviewer for excellent comments which improved the quality of our manuscript. VKJ acknowledges funding by ONR N000140510104 ATIP and Brain NRG JSMF22002082.

Appendix

A Nonlinear phase equations

Rewriting equations (4) and (5) as a second order ordinary differential equation we get

$$\ddot{x}_j = -x_j + a + c\dot{x}_j - c\frac{x_j^2}{R_0^2}\dot{x}_j + c\epsilon\dot{p}(1-p^2) \quad (16)$$

Furthermore, inserting (6) and applying the "slowly varying amplitude" and "rotating wave" approximations, we obtain

$$e^{i\omega t}[(1-\omega^2)A_j + 2i\omega\dot{A}_j - ci\omega A_j + ci\omega\frac{|A_j|^2}{R_0^2}A_j] = c\epsilon i\omega f(r, A_j, A_{j\tau}, A_j^*, A_{j\tau}^*, A_{k\tau}, A_{k\tau}^*) \quad (17)$$

where f represents a nonlinear complex-valued function. Separating real and imaginary parts yields the phase equation (9) and the amplitude equation

$$\begin{aligned} \frac{1}{c}\dot{R} = & \frac{1}{2}\left(R - \frac{R^3}{R_0^2}\right) + \frac{\epsilon}{2}\left[\sum_{l,m=1}^2 A_{lm} \cos(2\phi_{l\tau} - \phi_{m\tau} - \phi_j) + \right. \\ & \sum_{l,m=1}^2 B_{lm} \cos(\phi_{l\tau} - \phi_{m\tau} - 2\phi_j) + C \cos(\phi_{k\tau} - \phi_{j\tau}) + \\ & \left. \sum_{l,m=1}^2 D_{lm} \cos(\phi_{l\tau} + \phi_{m\tau} - 2\phi_j) + E \cos(\phi_{j\tau} + \phi_j)\right] \quad (18) \end{aligned}$$

Following the lines of Haken et al. (1985), the amplitude R can be adiabatically eliminated in the neighborhood of the phase instability, $\dot{R} \approx 0$, and yields $R_1 \approx R_2 = R_0$ for negligible influence of coupling. For completeness, we present the coefficients $A_{lm}, B_{lm}, C, D_{lm}$ and E for equations (9) and (18)

$$A_{11} = -1 + 4rR_0^2 + r + 5r^2R_0^2 - 3r^3R_0^2 \quad (19)$$

$$A_{12} = r(r-1)^2 R_0^2 \quad (20)$$

$$A_{21} = r^2(1-r) R_0^2 \quad (21)$$

$$A_{22} = (3r^3 R_0^2 - 4r^2 R_0^2 + 5r R_0^2 - r) R_0^2 \quad (22)$$

$$B_{11} = B_{22} = (1-r)^2 R_0^2 \quad (23)$$

$$B_{12} = 0 \quad (24)$$

$$B_{21} = 2r(r-1) R_0^2 \quad (25)$$

$$C = r(4r-3) R_0^2 \quad (26)$$

$$D_{11} = (1-r)^2 R_0^2 \quad (27)$$

$$D_{12} = D_{21} = r(1-r) R_0^2 \quad (28)$$

$$D_{22} = r^2 R_0^2 \quad (29)$$

$$E = 2R_0^2(r-1) \quad (30)$$

B Linear phase equation

B.1 Derivation of linear relative phase equations from the nonlinear individual phase equations:

Equation (9) can be written as,

$$\begin{pmatrix} \dot{\phi}_1 \\ \dot{\phi}_2 \end{pmatrix} = \begin{pmatrix} f_1(\phi_1, \phi_{1\tau}, \phi_{2\tau}) \\ f_2(\phi_2, \phi_{2\tau}, \phi_{1\tau}) \end{pmatrix} \quad (31)$$

The linearized system around fixed points is given by equation (10), where \mathbf{L}_1 and \mathbf{L}_2 are the Jacobian matrices. Since there is no dependence of ϕ_k terms in equation (9) one can immediately see that \mathbf{L}_1 is a diagonal matrix. The symmetry of the coupling is reflected in \mathbf{L}_2 via a symmetric matrix. Hence for both antiphase $\phi_1 - \phi_2 = \pi$ and inphase $\phi_1 - \phi_2 = 0$ the matrices \mathbf{L}_1 and \mathbf{L}_2 can be written as

$$\mathbf{L}_1 = \begin{pmatrix} L & 0 \\ 0 & L \end{pmatrix} \quad (32)$$

and

$$\mathbf{L}_2 = \begin{pmatrix} L_{1\tau} & L_{2\tau} \\ L_{2\tau} & L_{1\tau} \end{pmatrix} \quad (33)$$

where L , $L_{1\tau}$ and $L_{2\tau}$ are functions of r and R_0 . Introducing the relative phase variable $\phi = \phi_1 - \phi_2$ and $\phi_\tau = \phi_{1\tau} - \phi_{2\tau}$ and using equations (10, 32, 33) we obtain the equation (11) for relative phase where $L_\tau = L_{1\tau} - L_{2\tau}$ and L_τ is a function of r and R_0 . In the following sections, expressions for L and L_τ are derived for antiphase and inphase solutions.

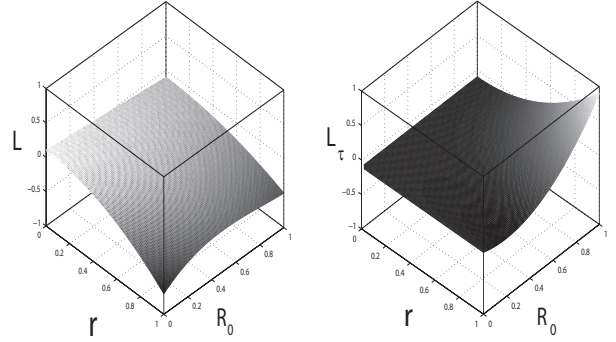


Figure 7 Nonlinearities of the coefficients L and L_τ for antiphase initial condition. a) L as a function of r and R_0 b) L_τ as a function of r and R_0 . Both functions are plotted for $\epsilon = 0.2$.

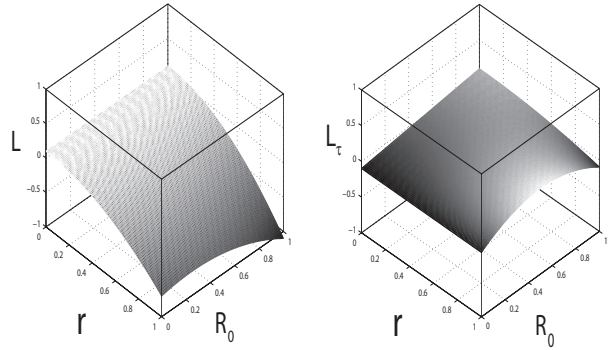


Figure 8 Nonlinearities of the coefficients L and L_τ for inphase initial condition. a) L as a function of r and R_0 b) L_τ as a function of r and R_0 .

B.2 Coefficients L and L_τ for antiphase

We obtain

$$L = \frac{\epsilon}{2} (1 - 2r - 8R_0^2 + 16rR_0^2 - 20r^2R_0^2 + 8r^3R_0^2) \quad (34)$$

and

$$L_\tau = \frac{\epsilon}{2} (-1 - 6rR_0^2 + 16r^2R_0^2) \quad (35)$$

For both cases $(\phi_1, \phi_2) = (\pi, 0)$ and $(0, \pi)$ the above expressions remain the same. We plot L and L_τ as functions of r and R_0 in Figure 7.

B.3 Coefficients L and L_τ for inphase

Here, we present the coefficients L , L_τ for inphase solutions.

$$L = \frac{\epsilon}{2} (1 - 8R_0^2 + 4rR_0^2 - 8r^2R_0^2) \quad (36)$$

$$L_\tau = \frac{\epsilon}{2} (-1 + 2r + 10rR_0^2 - 12r^2R_0^2) \quad (37)$$

We plot L and L_τ as functions of r and R_0 in Figure 8 for $\epsilon = 0.2$.

References

- Baraldi, P., Porro, C. A., Serafini, M., Pagnoni, G., Murari, C., Corazza, R., and Nichelli, P. (1999). Bilateral representation of sequential finger movements in human cortical areas. *Neuroscience Letters*, 269:95–98.
- Bernstein, N. (1967). *The coordination and regulation of movements*. England: Pergamon Press. Oxford.
- Bressler, S. and Kelso, J. A. S. (2001). Cortical coordination dynamics. *Trends in Cognitive Sciences*, 5:26–36.
- Brinkman, J. and Kuypers, H. G. J. M. (1972). Split-brain monkeys: Cerebral control of ipsilateral and contralateral arm, hand and finger movements. *Science*, 176:536–538.
- Brown, W. S., Jeeves, M. A., Dietrich, R., and Burnison, D. S. (1999). Bilateral field advantage and evoked potential interhemispheric transmission in commissurotomy and callosal agenesis. *Neuropsychologia*, 37:1165–80.
- Byblow, W. D., Carson, R. G., and Goodman, D. (1994). Expressions of asymmetries and anchoring in bimanual coordination. *Human Movement Science*, 13:3–28.
- Cardoso de Oliveira, S. (2002). The neuronal basis of bimanual coordination: Recent neurophysiological evidence and functional models. *Acta Psychologica*, 110:139–159.
- Cardoso de Oliveira, S., Gribova, A., Donchin, O., Bergman, H., and Vaadia, E. (2001). Neural interactions between motor cortical hemispheres during bimanual and unimanual arm movements. *European Journal of Neuroscience*, 14:1881–1896.
- Carson, R. G. (2005). Neural pathways mediating bilateral interactions between the upper limbs. *Brain Research Reviews*, 49(3):641–662.
- Carson, R. G., Riek, S., Smethurst, C. J., Parraga, J. F., and Byblow, W. D. (2000). Neuromuscular-skeletal constraints upon the dynamics of unimanual and bimanual coordination. *Experimental Brain Research*, 131(2):196–214.
- Cattaert, D., Semjen, A., and Summers, J. (1999). Simulating a neural cross-talk model for between-hand interference during bimanual circle drawing. *Biological Cybernetics*, 81:343–358.
- Cheyne, D., Endo, H., Takeda, T., and Weinberg, H. (1997). Sensory feedback contributes to early movement-evoked fields during voluntary finger movements in humans. *Brain Research*, 771(2):196–202.
- Clarke, J. M., Halgren, E., and Chauvel, P. (1999). Intracranial ERP recordings during a lateralized visual oddball task: II. Temporal, parietal and frontal recordings. *Electroencephalography and Clinical Neurophysiology*, 110:1226–1244.
- Clarke, J. M. and Zaidel, E. (1989). Simple reaction times to lateralized light flashes. varieties of interhemispheric communication routes. *Brain*, 112:849–870.
- Daffertshofer, A., Peper, C. E., and Beek, P. J. (2005). Stabilization of bimanual coordination due to active interhemispheric inhibition: a dynamical account. *Biological Cybernetics*, 92:101–109.
- Datko, R. (1978). A procedure for determination of the exponential stability of certain differential-difference equations. *Quarterly of Applied Mathematics*, 36:279–292.
- Debaere, F., Swinnen, S., Beatse, E., Sunaert, S., Hecke, P. V., and Duysens, J. (2001). Brain areas involved in interlimb coordination: A distributed network. *NeuroImage*, 14:947–958.
- Franz, E. A., Eliassen, J. C., Ivry, R., and Gazzaniga, M. S. (1996). Dissociation of spatial and temporal coupling in the bimanual movements of callosotomy patients. *Psychological Science*, 7:306–310.
- Friston, K., Harrison, L., and Penny, W. (2003). Dynamic causal modelling. *NeuroImage*, 19:1273–1302.
- Fuchs, A., Jirsa, V. K., and Kelso, J. A. S. (2000). Issues for the coordination of human brain activity and motor behavior. *NeuroImage*, 11:375–377.
- Georgopoulos, A. P., Lurito, J. T., Petrides, M., Schwartz, A. B., and Massey, J. T. (1989). Mental rotation of the neuronal population vector. *Science*, 243:234–236.
- Gerloff, C. and Andres, F. G. (2002). Bimanual coordination and interhemispheric interaction. *Acta Psychologica (Amst)*, 110(2-3):161–86.
- Gray, C. M., König, P., Engel, A. K., and Singer, W. (1997). Oscillatory responses in cat visual cortex exhibit intercolumnar synchronization which reflects global stimulus properties. *Nature*, 385:157–161.
- Grossberg, S. (1977). Pattern formation by the global limits of a nonlinear competitive interaction in n dimensions. *Journal of Mathematical Biology*, 4(3):237–56.
- Grossberg, S., Pribe, C., and Cohen, M. A. (1997). Neural control of interlimb oscillations 1. human bimanual coordination. *Biological Cybernetics*, 77:131–140.
- Haken, H. (1983). *Synergetics: An Introduction*. Springer Series in Synergetics. Springer-Verlag, 3 edition.
- Haken, H., Kelso, J. A. S., and Bunz, H. (1985). A theoretical model for phase transitions of human hand movement. *Biological Cybernetics*, 51:347–356.
- Hale, J. and Lunel, S. (1993). *Introduction to Functional Differential Equations*. Springer Verlag, NY.
- Halgren, E. (2004). How can intracranial recordings assist MEG source localization? *Neurology and Clinical Neurophysiology*, BioMag2004.
- Jantzen, K. J., Steinberg, G., and Kelso, J. A. S. (2004). Brain networks underlying human timing behavior. *Proceedings of National Academy of Sciences*, 101:6815–6820.
- Jirsa, V. K. (2004). Information processing in brain and behavior displayed in large-scale topographies such as EEG and MEG. *International Journal of Bifurcation and Chaos*, 14:679–692.

- Jirsa, V. K. and Ding, M. (2004). Will a large complex system with time delays be stable? *Physical Review Letters*, 93:070602:1–4.
- Jirsa, V. K. and Fuchs, A. (2000). The HKB model revisited: How varying the degree of symmetry controls dynamics. *Human Movement Science*, 19:425–449.
- Jirsa, V. K., Fuchs, A., and Kelso, J. A. S. (1998). Connecting cortical and behavioural dynamics: Bimanual coordination. *Neural Computation*, 10:2019–2045.
- Jirsa, V. K. and Haken, H. (1996). Field theory of electromagnetic brain activity. *Physical Review Letters*, 77:960–963.
- Jirsa, V. K. and Haken, H. (1997). A derivation of a macroscopic field theory of the brain from the quasi-microscopic neural dynamics. *Physica D*, 99:503–526.
- Jirsa, V. K., Jantzen, K. J., Fuchs, A., and Kelso, J. A. S. (2002). Spatiotemporal forward solution of the EEG and MEG using network modelling. *IEEE Transactions on Medical Imaging*, 21:493–504.
- Jirsa, V. K. and Kelso, J. A. S. (2003). Integration and segregation of perceptual and motor behavior. In Jirsa, V. K. and Kelso, J. A. S., editors, *Coordination Dynamics: Issues and Trends*, pages 243–259. Springer: Berlin, Heidelberg, New York.
- Jirsa, V. K. and Kelso, J. A. S. (2005). Excitator as the minimal model for discrete and rhythmic movement generation. *Journal of Motor behavior*, 37:35–51.
- Kay, B. A., Kelso, J. A. S., Saltzman, E. L., and Schöner, G. (1987). Space-time behavior of single and bimanual rhythmic movements: Data and limit cycle model. *Journal of Experimental Psychology: Human Perception and Performance*, 13(2):178–192.
- Kelso, J. A., Fuchs, A., Lancaster, R., Holroyd, T., Cheyne, D., and Weinberg, H. (1998). Dynamic cortical activity in the human brain reveals motor equivalence. *Nature*, 392(6678):814–8.
- Kelso, J. A., Holt, K. G., Rubin, P., and Kugler, P. N. (1981). Patterns of human interlimb coordination emerge from the properties of non-linear, limit cycle oscillatory processes: Theory and data. *Journal of Motor Behavior*, 13(4):226–61.
- Kelso, J. A. S. (1981). On the oscillatory basis of movement. *Bulletins of Psychonomic Society*, 18(63).
- Kelso, J. A. S. (1995). *Dynamic Patterns: The self-organization of brain and behaviour*. MIT Press, 1 edition.
- Kelso, J. A. S., Holt, K. G., Turvey, M. T., and Kugler, P. N. (1980). *Tutorials in motor behaviour*, chapter Coordinative structures as dissipative structures: II. Empirical lines of convergence. Amsterdam: North Holland.
- Kennerley, S. W., Diedrichsen, J., Hazeltine, E., Semjen, A., and Ivry, R. (2002). Callosotomy patients exhibit temporal uncoupling during continuous bimanual movements. *Nature Neuroscience*, 5:376–381.
- Kugler, P. N., Kelso, J. A. S., and Turvey, M. T. (1980). *Tutorials in motor behaviour*, chapter On the concept of coordinative structures as dissipative structures: I. Theoretical lines of convergence. Amsterdam: North Holland.
- Lee, T. D., Almeida, Q. J., and Chua, R. (2002). Spatial constraints in bimanual coordination: Influences of effector orientation. *Experimental Brain Research*, 146(2):205–12.
- Liepmann, H. (1920). *Apraxie*. Real-Encyclopedia der Gesamten Helkunde Ergebnisse der Gesamten Medizin Vol 1. Urban and schwarzenberg edition.
- Lim, K. O., Hedehus, M., Moseley, M., de Crespigny, A., Sullivan, E. V., and Pfefferbaum, A. (1999). Compromised white matter tract integrity in schizophrenia inferred from diffusion tensor imaging. *Archives of General Psychiatry*, 56(4):367–74.
- MacDonald, N. (1989). *Biological Delay Systems: Linear Stability Analysis*. Cambridge studies in mathematical biology; 8. Cambridge University Press.
- Marzi, C. A., Bisiacchi, P., and Nicoletti, R. (1991). Is interhemispheric transfer of visuomotor information asymmetric? Evidence from a meta-analysis. *Neuropsychologia*, 29:1163–77.
- McIntosh, A. R. (2004). Contexts and catalysts: A resolution of the localization and integration of function in the brain. *Neuroinformatics*, 2(2):175–82.
- Nagashino, H. and Kelso, J. A. S. (1992). Phase transitions in oscillatory neural networks. *Science of Artificial Neural Networks, International Society for Optical Engineering*, 1710:278–297.
- Nunez, P. L. (1974). The brain wave equation: A model for EEG. *Mathematical Biosciences*, 21:279–297.
- Penny, W., Ghahramani, Z., and Friston, K. J. (2005). Bilinear dynamical systems. *Philosophical Transactions of Royal Society B: Biological Sciences*, 360:983–993.
- Peper, C. E. and Beek, P. J. (1999). Modeling rhythmic interlimb coordination: The roles of movement amplitudes and time delays. *Human Movement Science*, 18:263–280.
- Robinson, P. A., Rennie, C. A., and Wright, J. J. (1997). Propagation and stability of waves of electrical activity in the cerebral cortex. *Physical Review E*, 56:826–840.
- Rokni, U., Steinberg, O., Vaadia, E., and Sompolinsky, H. (2003). Cortical representation of bimanual movements. *The Journal of Neuroscience*, 23:11577–86.
- Rouiller, E. M., Tanne, J., Moret, V., and Bossaoud, D. (1999). Origins of thalamic input to the primary, premotor and supplementary motor cortical areas and to area 46 in macaque monkeys: A multiple retrograde tracing study. *Journal of Comparative Neurology*, 409:131–152.
- Roxin, A., Brunel, N., and Hansel, D. (2005). Role of delays in shaping spatiotemporal dynamics of neuronal activity in large networks. *Physical Review Letters*, 94(23):238103.

- Sampaio, R. and Truwit, C. (2001). Myelination in the developing human brain. In Nelson, C. and Luciana, M., editors, *Handbook of Developmental Cognitive Neuroscience*. Bradford Books.
- Schmidt, R. (1975). A schema theory of discrete motor skill learning. *Psychological Review*, 86:225–260.
- Schmidt, R. C., Carello, C., and Turvey, M. T. (1990). Phase transitions and critical fluctuations in the visual coordination of rhythmic movements between people. *Journal of Experimental Psychology: Human Perception and Performance*, 16:227–247.
- Schmitz, D., Schuchmann, S., Fisahn, A., Draguhn, A., Buhl, E. H., Petrasch-Parwez, E., Dermietzel, R., Heinemann, U., and Traub, R. D. (2001). Axo-axonal coupling. a novel mechanism for ultrafast neuronal communication. *Neuron*, 31(5):831–40.
- Schöner, G. and Kelso, J. A. S. (1988). Dynamic pattern generation in behavioral and neural systems. *Science*, 239:1513–1519.
- Shampine, L. and Thompson, S. (2001). Solving DDEs in MATLAB. *Applied Numerical Mathematics*, 37:441–458.
- Sporns, O., Chialvo, D. R., Kaiser, M., and Hilgetag, C. C. (2004). Organization, development and function of complex brain networks. *Trends in Cognitive Sciences*, 8:418–425.
- Swinen, S. (2002). Intermanual crosstalk: From behavioural models to neural-network interactions. *Nature Neuroscience*, 3:350–361.
- Tass, P. (1999). *Phase resetting in medicine and biology*. Springer: Berlin, Heidelberg, New York.
- Temprado, J. J., Zanone, P. G., Monno, A., and Laurent, M. (1999). Attentional load associated with performing and stabilizing preferred bimanual patterns. *Journal of Experimental Psychology: Human perception and performance*, 25:1579–1594.
- Thorpe, S., Fize, D., and Marlot, C. (1996). Speed of processing in the human visual system. *Nature*, 381:520–522.
- Tuller, B. and Kelso, J. A. S. (1989). Environmentally specified patterns for normal and split brain subjects. *Experimental Brain Research*, 75:306–316.
- van Mourik, A. M., Daffertshofer, A., and Beek, P. J. (2006). Deterministic and stochastic features of rhythmic human movement. *Biological Cybernetics*, 94(3):233–44.
- Varela, F., Lachaux, J. P., Rodriguez, E., and Martinerie, J. (2001). The brainweb: phase synchronization and large-scale integration. *Nature Reviews Neuroscience*, 2:229–239.
- Wilson, H. R. and Cowan, J. D. (1972). Excitatory and inhibitory interactions in localized populations of model neurons. *Biophysical Journal*, 12(1):1–24.
- Wright, J. J. and Liley, D. T. J. (1995). Simulation of electrocortical waves. *Biological Cybernetics*, 72:347–356.
- Zanone, P. G. and Kelso, J. A. S. (1992). Evolution of behavioral attractors with learning: Non equilibrium phase transitions. *Journal of Experimental Psychology: Human Perception and Performance*, 18:403–421.